Physics Letters B 733 (2014) 366–372

Contents lists available at ScienceDirect

Physics Letters B

www.elsevier.com/locate/physletb

Observation of focusing of 400 GeV/c proton beam with the help of bent crystals

W. Scandale [a,b,e], G. Arduini [a], M. Butcher [a], F. Cerutti [a], S. Gilardoni [a], A. Lechner [a], R. Losito [a], A. Masi [a], E. Metral [a], D. Mirarchi [a], S. Montesano [a], S. Redaelli [a], G. Smirnov [a], L. Bandiera [c], S. Baricordi [c], P. Dalpiaz [c], V. Guidi [c], A. Mazzolari [c], D. Vincenzi [c], G. Claps [d], S. Dabagov [d], D. Hampai [d], F. Murtas [d], G. Cavoto [e], M. Garattini [e], F. Iacoangeli [e], L. Ludovici [e], R. Santacesaria [e], P. Valente [e], F. Galluccio [f], A.G. Afonin [g], Yu.A. Chesnokov [g], P.N. Chirkov [g], V.A. Maisheev [g,*], Yu.E. Sandomirskiy [g], I.A. Yazynin [g], A.D. Kovalenko [h], A.M. Taratin [h], Yu.A. Gavrikov [i], Yu.M. Ivanov [i], L.P. Lapina [i], W. Ferguson [j], J. Fulcher [j], G. Hall [j], M. Pesaresi [j], M. Raymond [j]

[a] CERN, European Organization for Nuclear Research, CH-1211 Geneva 23, Switzerland
[b] Laboratoire de l'Accelerateur Lineaire (LAL), Universite Paris Sud Orsay, Orsay, France
[c] INFN Sezione di Ferrara, Dipartimento di Fisica, Università di Ferrara, Ferrara, Italy
[d] INFN LNF, Via E. Fermi, 40 00044 Frascati (Roma), Italy
[e] INFN Sezione di Roma, Piazzale Aldo Moro 2, 00185 Rome, Italy
[f] INFN Sezione di Napoli, Italy
[g] Institute of High Energy Physics, Moscow Region, RU-142284 Protvino, Russia
[h] Joint Institute for Nuclear Research, Joliot-Curie 6, 141980 Dubna, Moscow Region, Russia
[i] Petersburg Nuclear Physics Institute, 188300 Gatchina, Leningrad Region, Russia
[j] Imperial College, London, United Kingdom

ARTICLE INFO

Article history:
Received 12 March 2014
Received in revised form 28 April 2014
Accepted 3 May 2014
Available online 9 May 2014
Editor: L. Rolandi

Keywords:
Bent crystal
Channeling
Focusing

ABSTRACT

The results of observation and studies of focusing of 400 GeV/c proton beam with the help of bent single crystals are presented. Two silicon crystals have been used in the measurements. The focal length of the first and second crystals is found to be 1.48 m and 0.68 m, respectively. The mean square size of the horizontal profile in the focus was 3.1 and 4.3 times as small as at the exit of the crystals.

1. Introduction

Particles channeled in a bent crystal are known to change their direction of motion. A common application of bent crystals for beam steering involves incident and outgoing beams with small divergence. On the other hand, a variation of the crystal shape and orientation can be instrumental in focusing and defocusing of the incident particle beam. The possibility of focusing of positive particle beams in bent crystals was first studied in Ref. [1] where experimental results on beam focusing are reported. Note that the crystal used in the experiment was rather thick and mounted in a heavy holder. However, such a design does not allow to use similar bent crystals in circulating accelerator beams. The proposed theoretical description of the method was restricted to geometrical relations.

In a new approach to the beam focusing with the help of bent single crystals [2] a simple description of the dependence of the mean square size of the beam on the distance from the crystal exit has been obtained. In particular, this description can be applied to calculations of beam focusing with a crystal of varying radius along the beam propagation direction. The technique developed for manufacturing bent single crystals with varying radius of curvature made it possible to construct a new device which did

* Corresponding author.
E-mail address: maisheev@ihep.ru (V.A. Maisheev).

http://dx.doi.org/10.1016/j.physletb.2014.05.010

not contain heavy parts. A theoretical description of particle beam focusing is presented in Ref. [2]. Experimental observation of the focusing effect produced by this device installed in a 50 GeV/c extracted proton beam at the IHEP accelerator has been reported in Ref. [3]. The beam coordinate distribution was obtained using a photo-emulsion method for the track position measurements.

This paper presents the results of studies of crystal focusing in a 400 GeV/c proton beam. The experiment was carried out at the H8 beam-line of the CERN Super Proton Synchrotron (SPS). Two silicon crystals manufactured using the technique described in [2] were used in studies of the focusing effect. High resolution coordinate detectors [4] which allowed to investigate the focusing process in detail were used for the precise tracking of the beam particles upstream and downstream of the bent crystal. The experiment profited from favorable background conditions and the use of electronic detectors which have an obvious advantage over the photo-emulsion method used in [3].

2. Beam focusing with bent crystals

2.1. Principle of beam focusing

Beam particles can be focused at a point if some specific conditions are fulfilled. The principle of focusing can be illustrated by the diagram in Fig. 1. A cut view of the crystal in the xz projection before it is bent is shown at the top.

The particle beam is directed along z axis and it is incident orthogonally on the face of the bent crystal. Under this condition, the particles are easily captured into the channeling mode. The end face of the crystal is fabricated with a special cut along the edge CD. Let us consider particles incident onto the crystal at the transverse coordinates x_1 and x_2 and captured in the channeling regime.

One can see that particles with different initial transverse coordinates have different paths in the body of a single crystal: $l_1(x_1)$ and $l_2(x_2)$, respectively. For particles with initial coordinates x_1 and x_2 the variations of angles (relative to the initial direction of motion) in the bending plane are $\varphi(x_1) = l_1(x_1)/R$ and $\varphi(x_2) = l_2(x_2)/R$, where R is the bending radius. Here we assume that the maximum bending angle of the single crystal $\varphi_{\max} \gg \theta_c$, where θ_c is the critical channeling angle. Then in this case we can neglect oscillations of particle angle due to the channeling process. It is easy to show that under appropriate conditions the two particle trajectories will intersect at some point (point O' in Fig. 1). The distance to the intersection point is determined by

$$L = -R(x_1 - x_2)/(l_1 - l_2). \tag{1}$$

Note that for a straight single crystal, that is before the crystal is bent, one can use the relation $z(x) = l(x)$, where $z(x)$ is the coordinate along the beam propagation direction. Under the condition that $(x_1 - x_2)/(z_1 - z_2) = const$ for any pair of coordinates (x_1, x_2), all trajectories of the channeling particles cross at the point O'. This means that the beam has a focus at the point O'. This consideration is rather simplified and does not take into account some features, for example, the variation of R along z axis. Moreover, the condition $(x_1 - x_2)/(z_1 - z_2) = const$ means that the projection of the crystal edge onto the x, z plane is a straight line (assuming R to be constant along z). In the general case, the crystal edge is described with a nonlinear function $F(x)$ which determines the position of the point (x, z) at the edge CD in Fig. 1.

2.2. Single crystals for experiment

For investigations of the focusing properties of bent single crystals the crystals should be fabricated by means of a special method [2]. The crystal which was fabricated for the present experiment is shown in Fig. 2. The upper part of the figure shows the cross section of the straight crystal which should be bent with the help of a special device. Let us introduce the Cartesian coordinate system (x, y, z) as shown in Fig. 2. The crystal is of a trapezoidal form in the x, z plane and has overall dimensions 0.9 (edge AB), 40, and 3 (edge AD) mm in the x, y, z directions, respectively. The edge CD is ≈ 0.4 mm. We show below that focusing takes place when the dependence $x = F(z)$ is approximately linear. In addition, when bending a strip of a trapezoidal shape one can expect that its bending radius will change along the z direction of such a deflector. This problem is considered theoretically in Ref. [2] where results of measurements of the bending radius in a similar deflector are also reported. The measured variation of bending radius along the z-coordinate can be described with the help of the empirical relation:

$$R(z) = \frac{R_0}{1 - Cz/L_0}, \tag{2}$$

where R_0 is the bending radius at $z = 0$, $L_0 = \mathrm{AD}$ is the single crystal thickness and $C = 0.8$ is the constant value. The deflection angle φ as a function of z for a single crystal with varying radius defined by Eq. (2) is written as follows:

$$\varphi(z) = \frac{z}{R_0} - \frac{Cz^2}{2L_0R_0}. \tag{3}$$

From this it follows that the full deflection angle (at $z = L_0$) is equal to $L_0/R_0(1 - C/2)$.

Two bent single crystals have been used in our experiment. The first crystal has a maximum deflection angle ≈ 0.3 mrad whereas for the second crystal it is ≈ 0.6 mrad. The measurements of the deflection angle performed in Ref. [2] at six points along z were used in calculations of the relative deflection angle displayed by points with error bars in Fig. 3. The curve 1 shown in Fig. 3 corresponds to the approximation of $\varphi(z)$ which used Eq. (3).

Note that in studies of its focusing properties a crystal cut to a triangular shape (triangle BCE in Fig. 2) should be used. However, we chose a trapezoidal shape in order to measure different features [2] in a single experiment. Due to this fact we consider below only one part of the crystal.

3. Description of beam focusing

We consider a crystal with an exit edge of arbitrary shape. The changes in the beam profile downstream of the crystal can be described as follows:

$$\sigma_x(l) = \int_0^d \rho(x)(X - \overline{X})^2 dx, \tag{4}$$

where $\sigma_x(l)$ and $X = x + \varphi l$ are the mean square size of the beam and the particle coordinate at the distance l in space between the crystal exit face and this point (assuming $l \gg L_0$), $\rho(x)$ is the distribution function over the x-coordinate normalized to unity at $z = L_0$, and $\overline{X} = \int_0^d \rho(x)(x + \varphi l)dx$. In the case when the crystal has a varying radius, the deflection angle is defined by the following relation:

$$\varphi(x) = \int_0^{F(x)} \frac{dz}{R(z)}. \tag{5}$$

As mentioned in Section 2.1, in the general case the variable upper limit of integration is defined as $z_{\max} = F(x)$, where the function

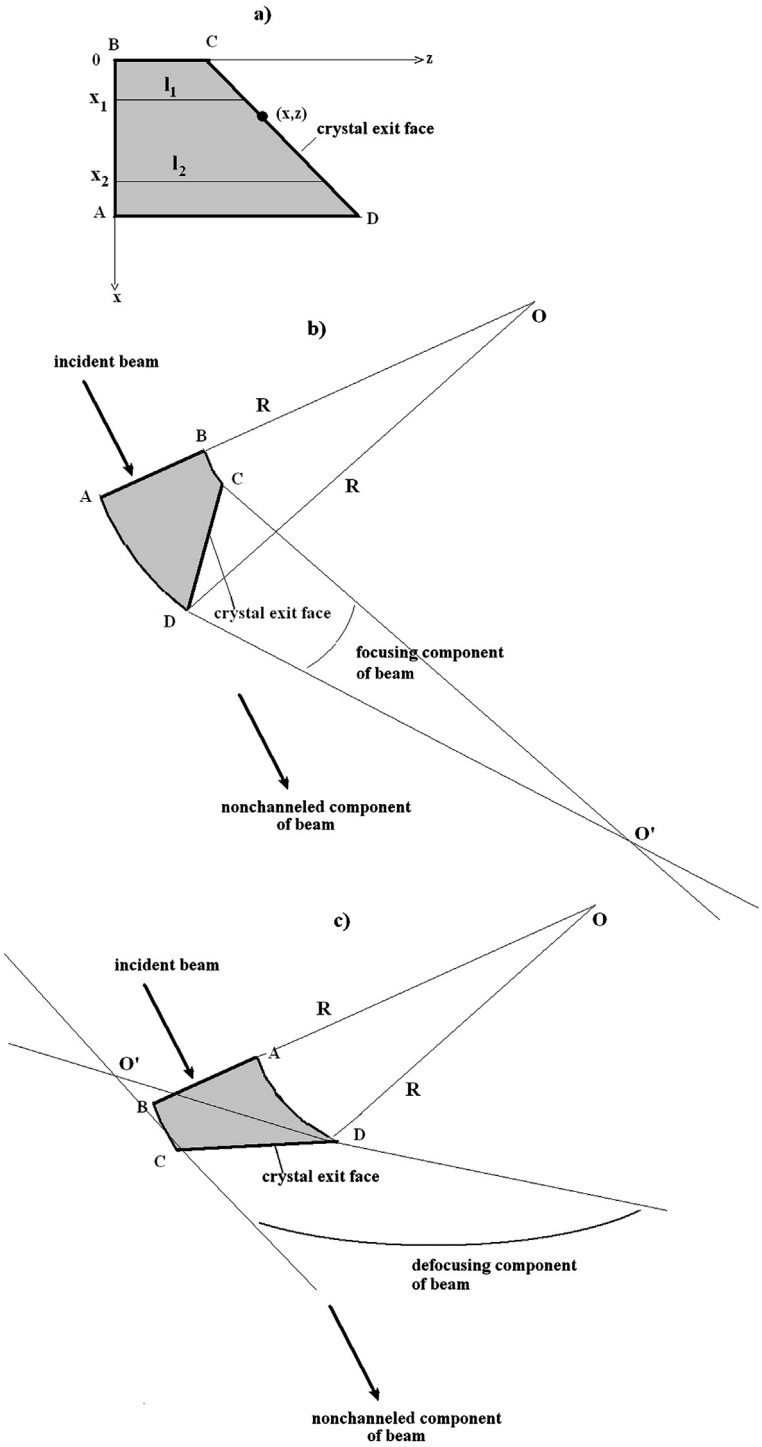

Fig. 1. (a) Geometry of a straight crystal, (b) the diagram showing the principle of beam focusing and (c) the diagram showing the principle of beam defocusing. Points O and O' correspond to the center of the bend and the focal point, respectively.

$F(x)$ is determined by the shape of the crystal edge. In the ideal case, the edge BC of the crystal is described with a linear equation $z = kx$, where k is determined from measurements. Then Eq. (3) is written as follows:

$$\varphi(x) = \frac{kx}{R_0} - \frac{Ck^2x^2}{2L_0R_0}, \tag{6}$$

where $R_0 = L_0(1-C/2)/\varphi_{\max}$ and $\varphi_{\max}$ is the maximum deflection angle.

Then one obtains

$$\sigma_x(l) = \langle x^2\rangle - \bar{x}^2 + \big(\langle\varphi^2\rangle - \bar{\varphi}^2\big)l^2 + 2\big(\langle x\varphi\rangle - \bar{x}\bar{\varphi}\big)l, \tag{7}$$

where $\langle x^2\rangle$ and $\langle\varphi^2\rangle$ are the mean square size of the beam and the mean square deflection angle at the exit face, $z = L_0$ ($l = 0$), $\bar{x}$ and $\bar{\varphi}$ are the mean size of the beam and the mean deflection angle (for $l = 0$), and $\langle x\varphi\rangle = \int_0^d x\varphi(x)\rho(x)dx$, and d is the transverse size of a single crystal which varies in this case from $x_{\min}$ to $x_{\max}$.

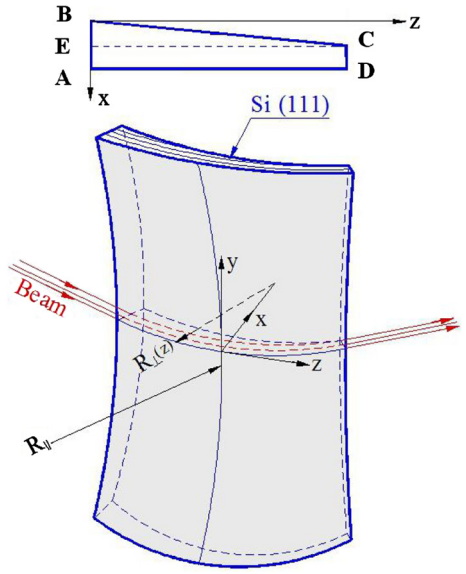

Fig. 2. The crystal deflector cut along the z axis. At the top, the cross section of a straight crystal is shown.

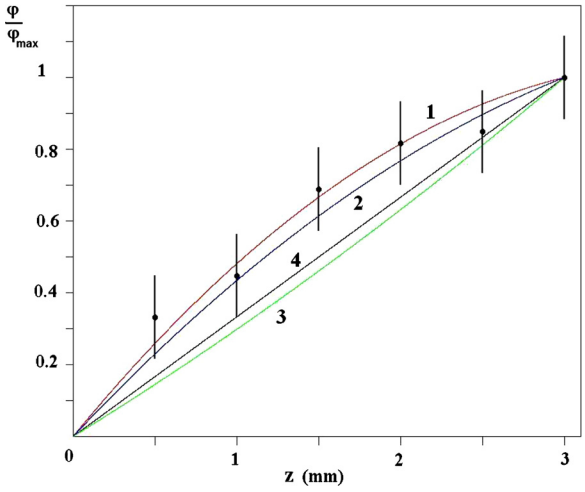

Fig. 3. The relative deflection angle as a function of coordinate z. The results of measurements for the first crystal are shown by filled circles with error bars. The curve 1 is the approximation $\varphi(z)/\varphi_{\max} = (z - Cz^2/(2L_0))/(L_0(1 - C/2))$ calculated for $C = 0.8$. The curves 2 and 3 are obtained by approximating the experimental data for the first and second crystals, respectively, with a second order polynomial. The curve 4 is the linear dependence ($C = 0$).

Now we can take into account the natural divergence of the beam due to the oscillating motion of particles in the channeling regime. This consideration is similar to the one of Ref. [5] where the overall distribution of particles can be represented as a convolution of two independent distributions.

Really, the sum distribution function over X-coordinate at the distance l is equal to $\rho_s(X,l) = \int_{-\infty}^{\infty} \rho_c(Y)\rho_X(X - Y)dY$, where $\rho_c(Y)$ is the distribution function over Y-variable ($Y = \theta l$) and $\rho_X(X)$ is the distribution function over X-coordinate ($dN = \rho(x)dx = \rho_X(X)dX$) with the mean square size $\sigma_x(l)$ (see Eq. (5)). All the distribution functions are normalized to unit. As a result, we get for the total mean square size

$$\sigma_T(l) = \sigma_x(l) + \left(\langle\theta^2\rangle - \bar{\theta}^2\right)l^2, \tag{8}$$

where $\langle\theta^2\rangle, \bar{\theta}$ are the mean square angle and mean angle of corresponding distribution.

The function $\sigma_T(l)$ has a minimum when

$$l = l_f = -\frac{\langle x\varphi\rangle - \bar{x}\bar{\varphi}}{\langle\varphi^2\rangle - \bar{\varphi}^2 + \langle\theta^2\rangle - \bar{\theta}^2}. \tag{9}$$

Beam focusing takes place if $l_f > 0$, which means that $\bar{x}\bar{\varphi} - \langle x\varphi\rangle > 0$.

4. Experimental set up

The experiment was carried out at the H8 beam-line of the CERN SPS using a practically pure 400 GeV/c proton beam for the measurements. The experimental layout was similar to that described earlier in Ref. [6]. A high precision goniometer was used to orient the crystal planes with the respect to the beam axis with an accuracy of 2 μrad. The accuracy of the preliminary crystal alignment using a laser beam was about 0.1 mrad. Five pairs of silicon microstrip detectors, two upstream and three downstream of the crystal, were used to measure incoming and outgoing angles of particles with an angular resolution in each arm of about 3 μrad [4]. The geometric parameters of the incident beam were measured with the help of the detector telescope. The width of the beam along the horizontal and vertical axes was several mm. The angular divergence of the incident beam in the horizontal and vertical planes was ∼10 μrad. The average cycle time of the SPS during the measurements was about 45 s with a pulse duration 10–11 s, with an average number of particles per spill of about $(1.3 \pm 0.1) \cdot 10^6$.

5. Results of measurements

In the experiment, the single crystal was oriented with the help of a standard procedure [7] which allowed to determine the range of goniometer angles corresponding to the channeling regime in the (111) plane for every crystal under study.

The results of measurements of x, φ-pairs are displayed in Fig. 4 for in the first (a) and second (b) crystals, respectively, for one orientation when the proton beam was captured in the channeling regime. Only a fraction of the events recorded was used in the study of the focusing process. These events are shown in Fig. 4 by red dots. The origin of the Cartesian coordinate system is located at point B (see Fig. 2). A significant number of events with small deflection angles (≤ 0.03 mrad) correspond to the non-channeling fraction of the beam.

The following selection criteria for the x and φ coordinates were used:

(1) they should satisfy the condition: 0.08 mm $\leq x \leq$ 0.48 mm and 0.08 mm $\leq x \leq$ 0.46 mm, for the first and second crystals, respectively;
(2) the deflection angles should be larger than 0.03 mrad;
(3) the non-channeling and dechanneling beam fractions (thin straight line in Fig. 4) should be removed.

Due to the overlap between channeling and non-channeling particles at small deflection angles, events reconstructed to be close to the face of the crystal with coordinates $0 < z < 0.08$ mm were excluded from the study.

By inspecting Fig. 4, one observes two unexpected features of channeling. The first is events clustering around certain x-coordinates. We explain this by the discrete character of measurements by the microstrip detectors because the width of each cluster is approximately equal to the width of a detector element. The second feature is manifested in a wide spread of exit angles at a fixed coordinate x. The observed spread is about a factor three larger than the critical channeling angle which determines the spread of

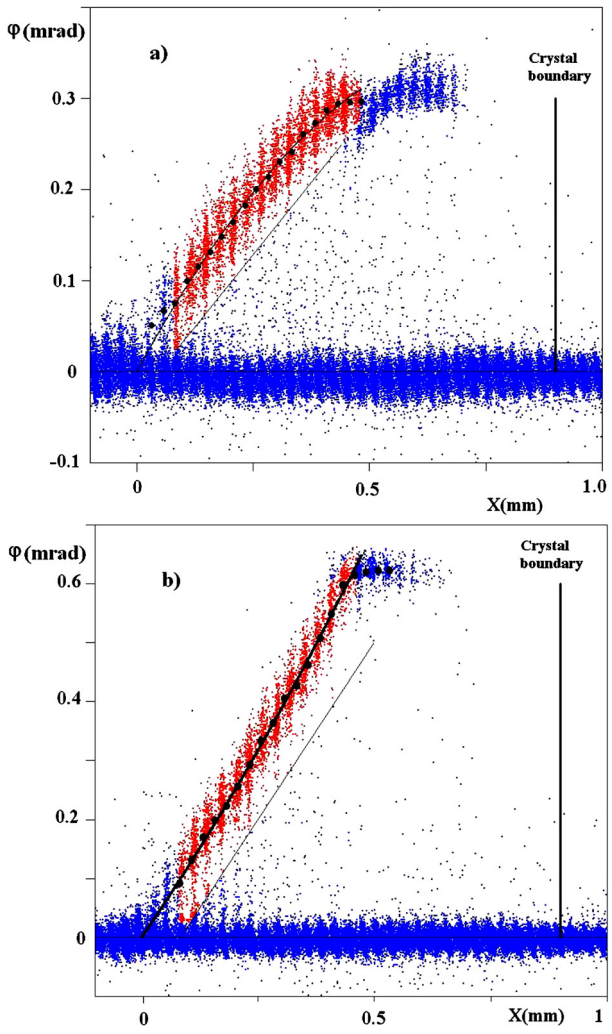

Fig. 4. Measurements of the correlations between $\varphi(x)$ and x for the first crystal (a) and for the second crystal (b). An approximation of the data with a second order polynomial is shown with the solid line. Filled circles correspond to the mean value of the distribution of the events in narrow intervals of x. (For interpretation of the references to color, the reader is referred to the web version of this article.)

exit angles in the ideal crystal. The latter feature can lead to larger uncertainties in reconstructing the beam profile. A list of effects which can potentially contribute to the angular distribution pattern is as follows:

(1) oscillating motion in channeling mode;
(2) torsion of a bent crystal;
(3) errors in measuring angles;
(4) fluctuation of $l(x)$ due to surface roughness (in a small area of fixed x).

It is easy to check that the second effect in the list does not change the result significantly. To verify this we selected events by reducing the size of the interval along y (the vertical coordinate) by a factor of 2 and 3 and found that the angular distributions remained practically unchanged.

Experimental points (red dots in Fig. 4) have been approximated with a second order polynomial in the form $\varphi(x) = ax + bx^2$ by using the least-squares method. The result obtained is shown in Fig. 4 by the thick solid line. The parameters of the fit are $a = (9.41 \pm 0.5) \cdot 10^{-4}$ mm^{-1}, $b = -(6.14 \pm 1.0) \cdot 10^{-4}$ mm^{-2}, and $a = (1.15 \pm 0.05) \cdot 10^{-3}$ mm^{-1}, $b = (4.65 \pm 1.0) \cdot 10^{-4}$ mm^{-2} for the first and second crystals, respectively.

It can be shown that similar results are obtained with an alternative procedure for the analysis in which φ is determined as the mean value of the distribution of experimental points in a narrow (≈ 0.025 mm) interval of the coordinate x. The results are displayed in the same plot with filled circles. The standard deviation of the angular distribution is determined as 22.5 μrad and 33 μrad for the first and second crystals, respectively.

It is obvious that knowing the coordinates x and φ allows reconstruction of the horizontal phase space and beam profile at any point downstream of the crystal deflector. Specifically, $X(l) = X(0) + \varphi l$, where $X(l)$ is the horizontal coordinate of the particle at a distance l downstream of the crystal.

Another important characteristic of the beam is its envelope which may be defined as the mean square size of beam at a distance l from the crystal exit. We can reconstruct the beam profile and find its mean square size and hence we can find the beam envelope. However, in our case an alternative approach can be used. In accordance with Eq. (7) we can find the envelope if the following three values are known from the experiment: $\langle x^2 \rangle - \bar{x}^2$, $\langle \varphi^2 \rangle - \bar{\varphi}^2$, and $\langle x\varphi \rangle - \bar{x}\bar{\varphi}$. Our analysis proves that the two methods are equivalent.

The results of reconstruction of the horizontal beam profile and its envelope are displayed in Figs. 5 and 6. One can clearly see the focusing effect for two crystals. For the first crystal, the focal length is 148 cm and the size of the beam at the focal point is 3.1 times smaller than at the crystal exit ($l = 0$). The analogous values for the second crystal are 68 cm and 4.3 times smaller.

6. Discussion

Below we compare the experimental results with features of the focusing anticipated from theoretical considerations.

In calculations which follow, a uniform beam distribution over the horizontal coordinate x is assumed at the exit of the crystal, $l = 0$. In this case the beam distribution function $\rho(x) = 1/(X_{\max} - X_{\min})$ and the mean square coordinate is equal to $\sigma_x(0) = (X_{\max} - X_{\min})^2/12$, where $X_{\max}$ and $X_{\min}$ are the maximum and minimum coordinates of particles. For the minimum coordinate we choose $X_{\min} = 0.08$ mm, and for the maximum one, $X_{\max} = 0.48$ mm and 0.46 mm for the first and second crystals, respectively. One finds good agreement between calculated values $s_x = \sqrt{\sigma_x} = 0.115$ mm (the first crystal) and 0.110 mm (the second crystal) with the measurement results 0.114 ± 0.007 mm and 0.104 ± 0.007 mm, respectively.

We calculated the envelopes for both crystals using with Eq. (6) and Eq. (7) (see the curve 2 in Figs. 5, 6). For calculation we use $C = 0.8$ as found in the measurements. It is important that in these calculations we also use Eq. (8) where for $\langle \theta^2 \rangle$-value we took the corresponding measured values (22.5 μrad and 33 μrad).

Note that the presence of the non-zero term with $C \neq 0$ in Eq. (6) corresponds to the varying curvature of the crystal (assuming an ideal shape of the cut). The case $C = 0$ refers to a bent crystal of constant radius $R = R_0 = L_0/\varphi_{\max}$. The calculations describing this particular case are shown by curve 3 in Figs. 5, 6.

Beam envelopes are calculated with a second order polynomial by fitting experimental data. The results are shown in Figs. 5, 6 by curve 4. One can see that curves 4 are in better agreement with experimental results than other curves (the curves 1 and 4 in Fig. 5 are very similar).

As pointed above, the scattering angle (at fixed coordinate) is several times larger than expected which we explain by the surface roughness. The fabrication of crystal deflectors with better surface quality is expected to improve beam focusing. For the ideal crystal,

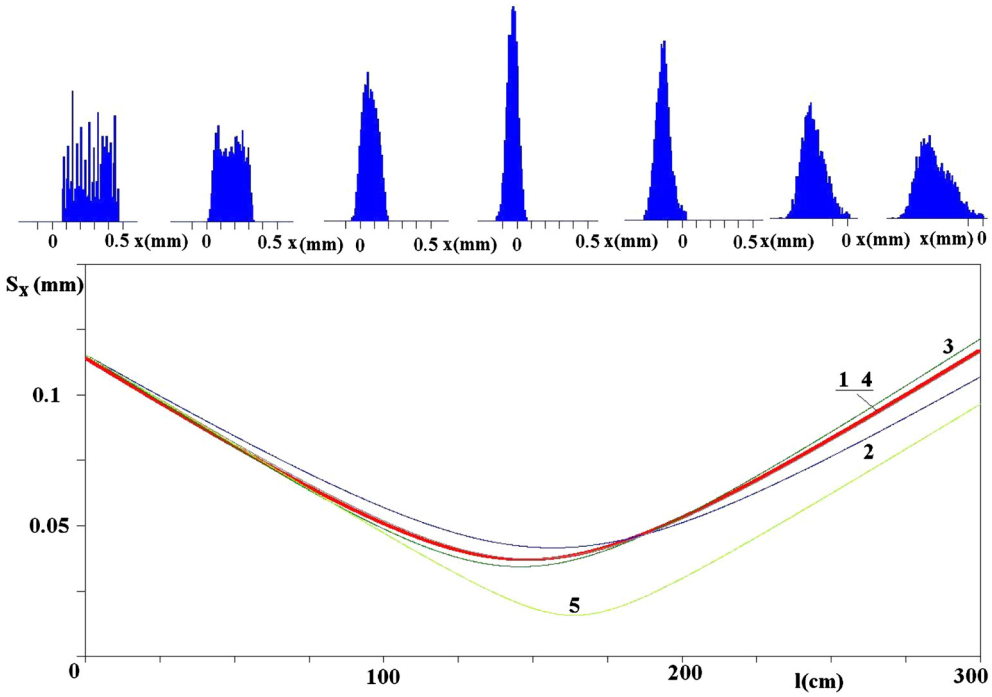

Fig. 5. The reconstructed measured profiles and envelope (the curve 1) of the beam for the first crystal. The curves 2–5 are calculations, for additional information, see text.

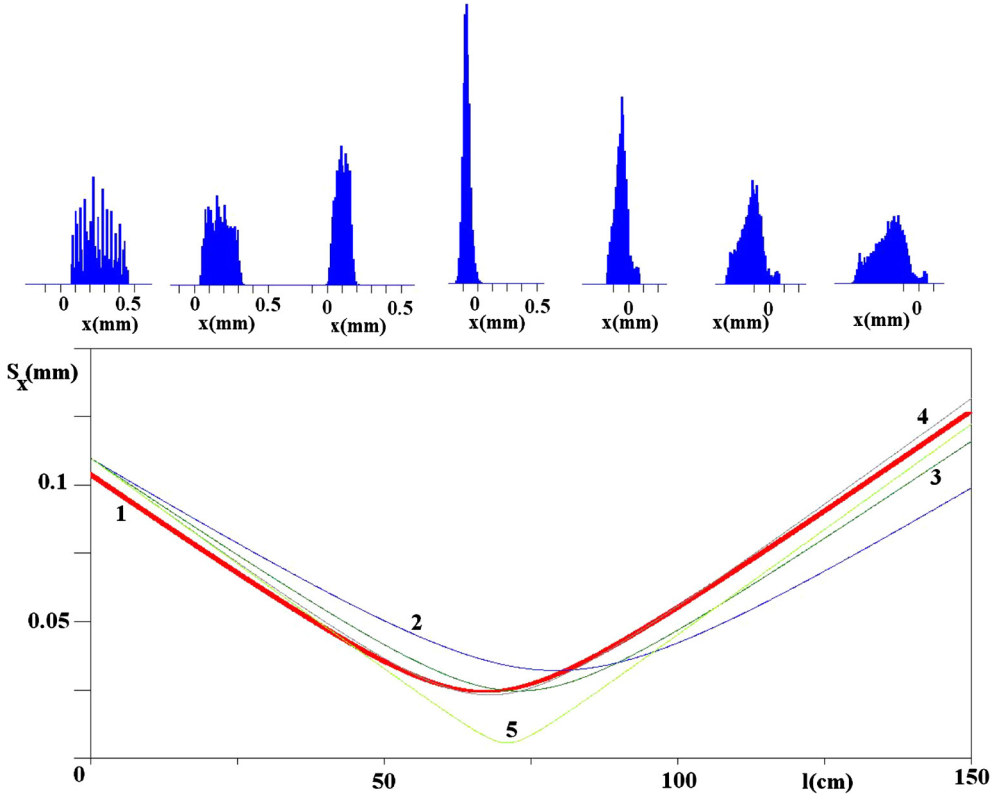

Fig. 6. The reconstructed measured profiles and envelope (the curve 1) of the beam for the second crystal. The curves 2–5 are calculations, for additional information, see text.

the minimum scattering angle (mean square) is about $\theta_c^2/3$. The curve 5 in Figs. 5, 6 corresponds to calculations of the beam envelope for the ideal surface of a crystal deflector.

We also investigated the case of the best description of the experimental data by a linear function $\varphi(x) = ax$. We find that this takes place for $a = 0.000719$ mm^{-1} and 0.00131 mm^{-1} for the first and the second crystals, respectively. Assuming $a = k/R_0$ (see Eq. (6)) we find that $k = 7.19$ and 6.55 for the first and second crystals, respectively. On the other hand, if k is determined from the ratio $L_0/X_{\max}$, $k = 6.25$ and 6.52 for the first

and second crystals, respectively. This result indicates that the second crystal can be approximated with a linear dependence on x whereas for the first crystal a linear approximation cannot be used. Moreover, the maximum deflection angle $\varphi_{\max}$ evaluated with $a = 0.000719$ mm^{-1} significantly exceeds the corresponding measured angle (0.000345 instead of 0.0003).

Fig. 3 illustrates the behavior of the deflection angle as a function of crystal length z. The curves were obtained by assuming that the edge of the crystal is a linear function of x. The curves 2 and 3 correspond to the parameters found for the curve 4 in Figs. 5 and 6, respectively. The data points show the results of measurements of a local crystal curvature carried out with the help of a laser. The measurements are available for the first crystal only. One can see that the curves 1 and 2 are in good agreement with experimental points. The curve 3 corresponds to the second crystal and it is close to the linear dependence of $\varphi(x)$ displayed by the curve 4.

Finally, we can use the obtained previously values of parameters a and b for determining the bending radius R_0 and the constant C introduced by Eq. (2). To this end one has to relate a and b to the first and second terms of Eq. (6), respectively, which yields $a = k/R_0$ and $b = Ck^2/(2L_0R_0)$. From these relations one finds $R_0 = 6.64 \pm 0.37$ m, $C = 0.65 \pm 0.15$ and $R_0 = 5.65 \pm 0.27$ m, $C = -0.37 \pm 0.1$ for the first and second crystals, respectively. Hence, the parameter C was found with the help of two methods: (1) from laser measurements and (2) from an experiment in the proton beam yielding the results which are in agreement within experimental errors. As a result, the curves 1 and 2 in Fig. 3 calculated with the obtained parameters pass close to each other. The cause of the difference between the first and second crystals is likely due to the different bending force (and hence C is a function of R_0, for example). Another explanation for the difference could be found in different methods of crystal fabrication. Specifically, the two crystals were identical in shape before bending, but the actual bending angles are different. Moreover, the side of the trapezoid corresponding to the exit face was processed differently in two crystals but with similar roughness of about 1 mkm. In particular, the diamond blade moved in the direction of the particle trajectory and in the transverse direction for the first and second crystals, respectively. Basically, the different calculations presented in Figs. 5 and 6 provide a good description of the focusing.

The focusing property of the developed bent crystals can be applied at the LHC and other high-energy accelerators and colliders for pursuing the research of processes in specific kinematic regions where emission angles of the secondary particles are small. The crystal can be aligned on a fixed target by focusing end face. Rotating the crystal about the axis one can deflect the particles from the target away from the adverse background region near the circulating beam. In this way, the crystal can create clean conditions for registration of secondary particles. Similar scheme can be suggested for production of secondary particle beams by employing relatively simple technique.

In some applications, beam defocusing can be required. It is expected, for instance, that this property of a bent crystal can improve the efficiency of the cleaning system by suppressing the beam halo in proton or ion colliders. The schematic diagram in Fig. 1(c) shows how a parallel beam can be transformed into a divergent one by employing a bent crystal.

7. Conclusions

The focusing of the channeling fraction of the incident particle beam in the bent crystal with a special cut has been observed. The r.m.s. beam width in the horizontal plane has been reduced in experiments with two crystals by factors of 3.1 and 4.3. The results of the measurements are in good agreement with theoretical predictions which use a relatively simple mathematical description of focusing. A fabrication method of the focusing crystals is proposed.

Acknowledgements

We acknowledge support from the Russian Foundation for Basic Research grant RFBR-CERN 12-02-91532 and the RF President Foundation grant SS-393.2012.2.

G. Cavoto, F. Iacoangeli and R. Santacesaria acknowledge the support from MIUR (grant FIRB RBFR085M0L_001/I11J10000090001).

References

[1] M.A. Gordeeva, M.P. Gur'ev, A.S. Denisov, et al., JETP Lett. 54 (1991) 487–490.
[2] A.G. Afonin, V.T. Baranov, M.K. Bulgakov, E.V. Lobanova, I.S. Lobanov, A.N. Luníkov, V.A. Maisheev, I.V. Poluektov, Yu.E. Sandomirskii, Yu.A. Chesnokov, P.N. Chirkov, I.A. Yazynin, Instrum. Exp. Tech. 56 (2) (2013) 123, http://dx.doi.org/10.1134/S0020441213010144, arXiv:1203.5586 [physics.acc-ph].
[3] A.G. Afonin, V.I. Baranov, V.T. Baranov, G.I. Britvich, A.P. Bugorskiy, M.K. Bulgakov, Y.A. Chesnokov, P.N. Chirkov, et al., JETP Lett. 96 (2012) 424;
A.G. Afonin, V.I. Baranov, V.T. Baranov, G.I. Britvich, A.P. Bugorskiy, M.K. Bulgakov, Y.A. Chesnokov, P.N. Chirkov, et al., Pisma Zh. Eksp. Teor. Fiz. 96 (2012) 470 (in Russian).
[4] M. Pesaresi, W. Ferguson, J. Fulcher, G. Hall, M. Raymond, M. Ryan, O. Zorba, J. Instrum. 6 (2011) P04006, http://dx.doi.org/10.1088/1748-0221/6/04/P04006.
[5] V.A. Maisheev, Phys. Rev. ST Accel. Beams 10 (2007) 084701, arXiv:physics/0607009.
[6] W. Scandale, G. Arduini, R. Assmann, F. Cerutti, S. Gilardoni, J. Christiansen, E. Laface, R. Losito, et al., Phys. Lett. B 701 (2011) 180.
[7] W. Scandale, A. Vomiero, S. Baricordi, P. Dalpiaz, M. Fiorini, V. Guidi, A. Mazzolari, G. Della Mea, et al., Phys. Rev. Lett. 101 (2008) 164801.